Materials Research Proceedings 41 (2024) 2210-2219 https://doi.org/10.21741/9781644903131-243

A robust identification protocol of flow curve adjusting parameters using uniaxial tensile curve

LEMOINE Xavier[1,a*], MUNIER Rémi[1,b] and BELLUT Xavier[2,c]

[1] Global R&D ArcelorMittal Maizières, voie Romaine, BP30320, F-57283 Maizières-lès-Metz, France

[2] Global R&D ArcelorMittal Montataire, 1 Route de Saint-Leu, F-60160 Montataire, France

[a]xavier.lemoine@arcelormittal.com, [b]remi.munier@arcelormittal.com, [c]xavier.bellut@arcelormittal.com

Keywords: Large Strain, Steel, Hardening Curve, Formability

Abstract. ArcelorMittal is constantly developing new steel grades to enable the automotive industry to offer safer, lighter, and more environmentally friendly vehicles. These new grades include advanced high-strength steels (AHSS) and Ultra High Strength steels (UHSS) having for some of them lower uniform elongation (UE) than conventional drawing steels. This particularity needs to be considered for an accurate formability prediction in sheet forming numerical simulations. One of these difficulties is the effect of the relatively low uniform elongation on the identification of the parameters of the isotropic hardening model. Various experimental tests can be used to reach the large plastic deformation (hydraulic bulge test, stack compression test, shear test, torsion test or plane strain compression test). The identification protocol of ArcelorMittal for hardening models is based solely on stress-strain curves determined in uniaxial tension. The Exp_S hardening law (TU experimental values before UE%, Swift extension above) was validated by comparison with the stress-strain curves obtained from measurements of experimental tests reaching large strains.

Introduction

The new advanced high-strength steels (AHSS) and Ultra High Strength steels (UHSS) for the automotive industry to improve weight reduction and passive safety result in lower uniform elongation than conventional drawing steels. In general, strain hardening laws are identified from the stress-plastic strain curve obtained from the uniaxial tensile test. Five measurements points on a B-pillar stamping part for seven steels with uniform elongation ranging from 2% to 14% (Figure 1) exceed the strain of the uniform elongation, sometimes to more than 12 times this strain where β is:

$$\beta = \frac{Measured\ strain}{Strain\ of\ Uniform\ Elongation} \quad (1)$$

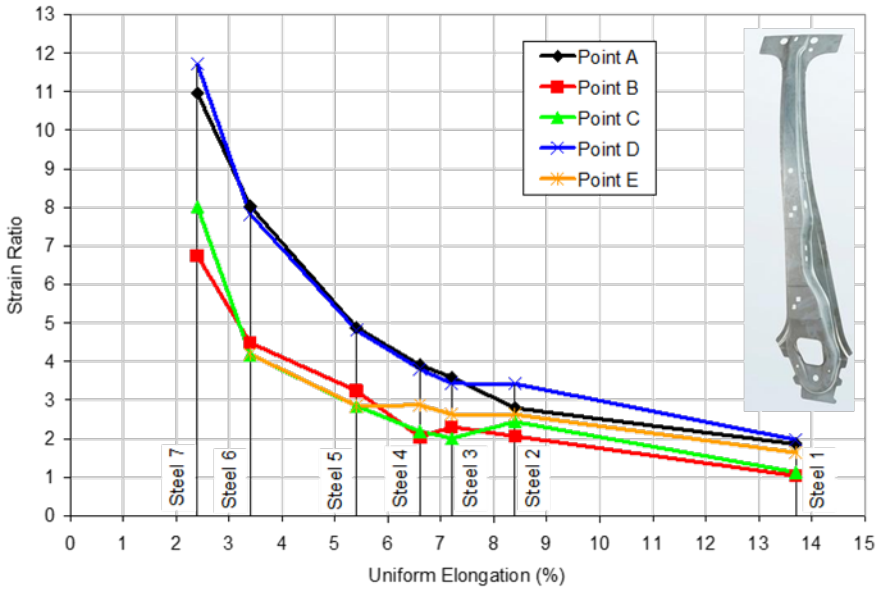

Figure 1 – Five measurements points on a B-pillar stamping part for seven steels with uniform elongation ranging from 2% to 14% exceed the strain of the uniform elongation.

There are 2 possible ways for a hardening model to correctly represent the stress-strain curve in large deformation [1], using tests to reach such strain levels:

- First way: to identify isotropic hardening parameters with the true stress-plastic strain curve obtained from these experimental tests allowing to reach large deformations [2].
- Second way: to identify isotropic hardening parameters with uniaxial tensile test and to choose the better prediction after uniform elongation with another rheological tests enabling to reach larger deformations [3].

Different large plastic strain experimental tests

Different experimental tests (cf. figure 2) allow to reach large plastic strain levels. Figure 3 shows the β-values (eq.1) achieved for these various experimental tests on different steel grades (Uniform elongation between 3% to 27% with thickness between 0.5 to 3 mm). Each point corresponds to a test, the majority of which comes from a publication [3 to 13]. Each of these tests has its advantages, disadvantages, and limitations (cf. table 1):

a) Uniaxial Tensile Test with local measure (UTT + DIC) [1, 4]: Based on a standard uniaxial tensile test coupled with digital image correlation for strain measurement, it is possible to decrease the measured length of 80 mm to 1 mm or less. As long as the deformation is constant over the width of the specimen, the local stress remains uniform and can be deduced from the tensile stress. Strains range between 0.2 and 0.4 can be reached depending on the material.

b) Shear Test (ST) [1]: The planar simple shear test device consists of two rigid bodies subjected to a parallel movement. With a high-resolution optical technique, the shear strain γ is deduced from the change in slope of an initially straight line or with digital image correlation. The shear stress is deduced by the shearing force F divided by the length l and by the sheet thickness t. The comparison of the shear flow curve with the tensile flow curve needs to generate an equivalent stress and equivalent strain. Depending on sheet thickness and material, sometimes the test is limited by fracture or buckling. Strains range between 0.1 and 0.5 can be reached.

c) Stack Compression Test (SCT) [1, 4]: The test consists of stacking a number of sheet specimens and compressing the stack using platens. The procedure adopted by An and

Vegter [14] reduces friction between each platen. The comparison of the stacked compression flow curve with the tensile flow curve needs to generate an equivalent stress and equivalent strain. Strains range between 0.2 and 0.3 can be reached before "barreling" effect. Using two video systems to characterize the anisotropy of a stacked compression test, M. Merklein [15] obtains a value of 0.5 despite the "barreling" effect.

d) Hydraulic Bulge Test (HBT) [1, 4]: This test deforms sheet specimen under action of hydraulic pressure through circular die. The state of stress can be determined analytically according to membrane theory using pressure, radius of curvature and thickness at the top of the dome. The bi-axial strains are measured with digital image correlation. The comparison of the equi-biaxial flow curve with the tensile flow curve needs to generate an equivalent stress and equivalent strain. Sometimes the test is limited by fracture or maximal pressure. Strains range between 0.5 and 0.7 can be reached.
e) In-plane Torsion Test (ITT) [4]: The in-plane torsion test is a shear test for sheet metals. A circular specimen is clamped at the center as well as on the outer rim. By imposing a different rotational movement between outer and inner clamping, the annular free area between the clamping devices is loaded under simple shear in the sheet plane. The shear stress can be deduced from the measured external torque. Shear strain can be calculated from the change in slope of an initially straight line or with digital image correlation. The comparison of the shear flow curve with the tensile flow curve needs to generate an equivalent stress and equivalent strain. According to the geometry of specimen groove, strains reach more than 0.5. Sometimes the test is limited by wrinkling instability or fracture.
f) Plane Strain Compression Test (PSCT) [4]: A rectangular sample of the sheet is compressed through the sheet thickness between two dies. The stress and strain fields determined analytically are based on the load and die displacement measurements, taking into account the friction influence. The comparison of the plane strain compression flow curve with the tensile flow curve needs to generate an equivalent stress and equivalent strain. Strains reach more than 0.3. Sometimes the test is limited by fracture.
g) Uniaxial Tensile Test on pre-rolled flat (UT on pre-rolled) [1]: Sheets (cold rolled and annealed) of several material types are rolled on an experimental mill several times up to specified thicknesses. Afterwards standard tensile tests are carried out on these pre-rolled specimens. The stress strain response of pre-strained test samples is obtained. The amount of pre-strain is assumed by the thickness reduction of the rolled samples - the deformation induced by rolling is not uniaxial compression in the thickness direction, but it is assumed to be a compressive deformation in plane strain with the plastic strain being zero in the width direction of the samples. Strains reach more than 0.7.

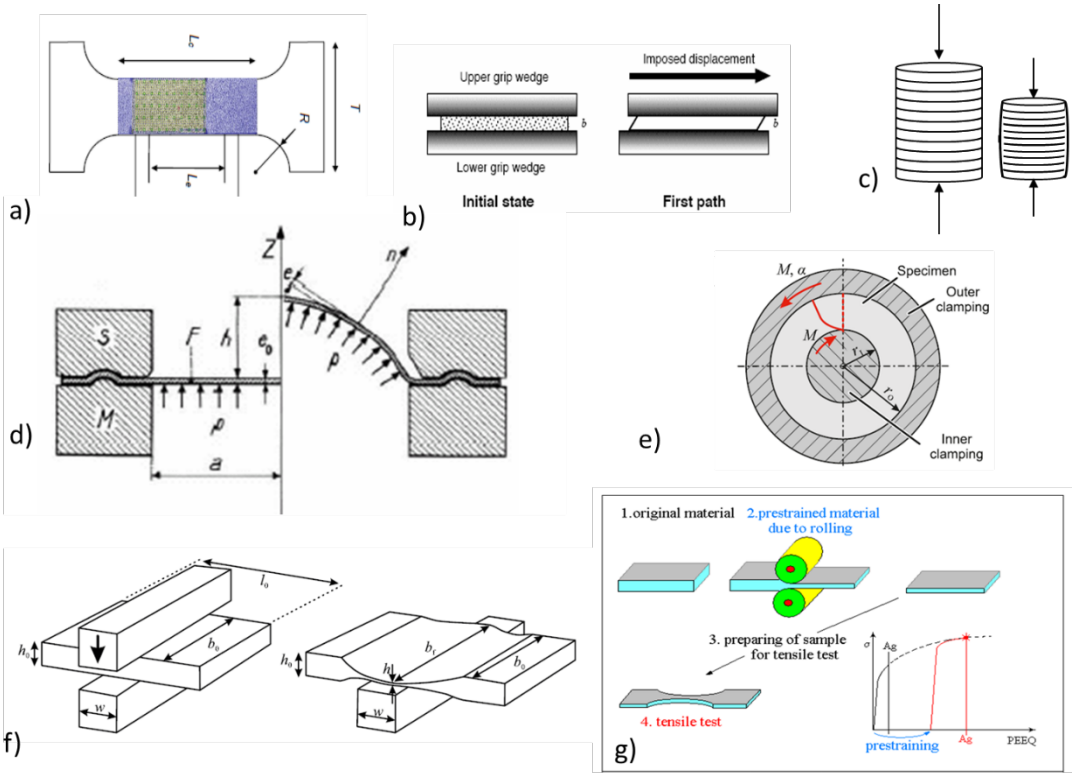

Figure 2 – Different experimental tests allowing to reach large plastic strain levels: a) Uniaxial Tensile Test with Local Measure [1], b) Shear Test [1], c) Stacked Compression Test [1], d) Bulge Test [1], e) In-plane Torsion Test [4], f) Plane Strain Compression Test [4] and g) Uniaxial Tensile Test on pre-rolled Flat [1].

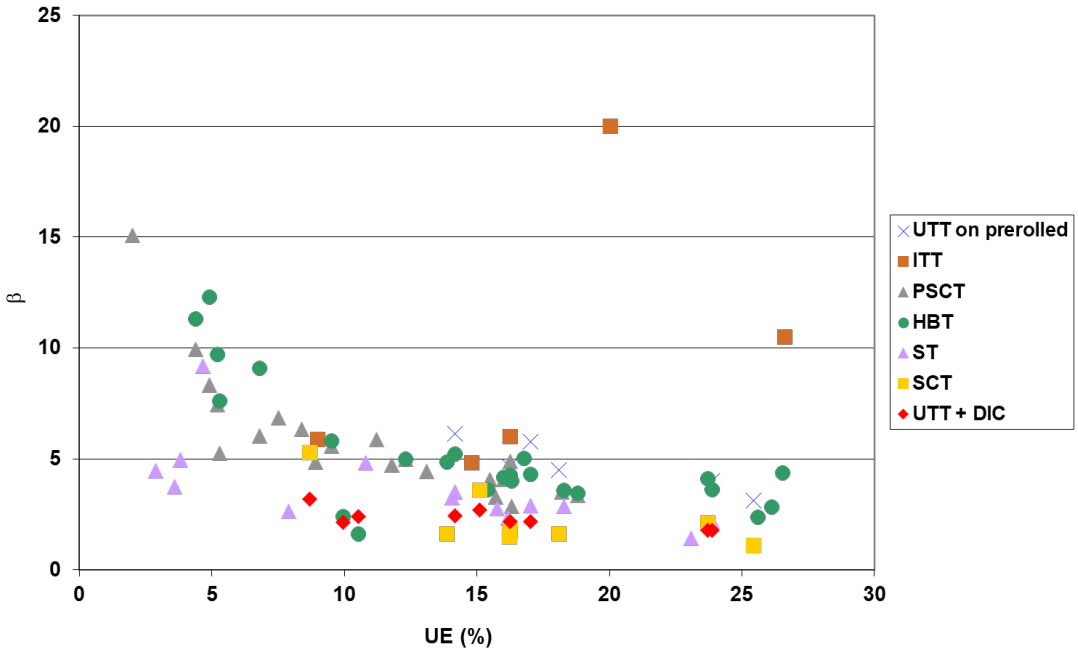

Figure 3 – β-values (eq.1) achieved for various experimental tests on different steel grades (Uniform elongation between 3% to 27% with thickness between 0.5 to 3 mm).

Table 1 – Different Experimental Tests regarding Standard Uniaxial Tensile Test (Standard UTT)

Experimental tests	β (eq. 1 and figure 3)	Sheet Surface Used Ratio	Complexity of Specimen Geometry	Test Duration Ratio
Standard UTT	1	1	-	1
UTT + DIC	1.5 to 2.5	1	Identic	1.5
ST	1.5 to 5	0.75	Simpler	1.5
SCT	2 to 4	0.5	Simpler	1
HBT	More 2.5	15	Simpler	3
ITT	More 4.5	1.5	More complex	1.5
PSCT	More 3	0.5	Simpler	1
UT on pre-rolled (10 pts)	More 3	15	Identic	10 + tooling

Flow curves comparison for different experimental tests

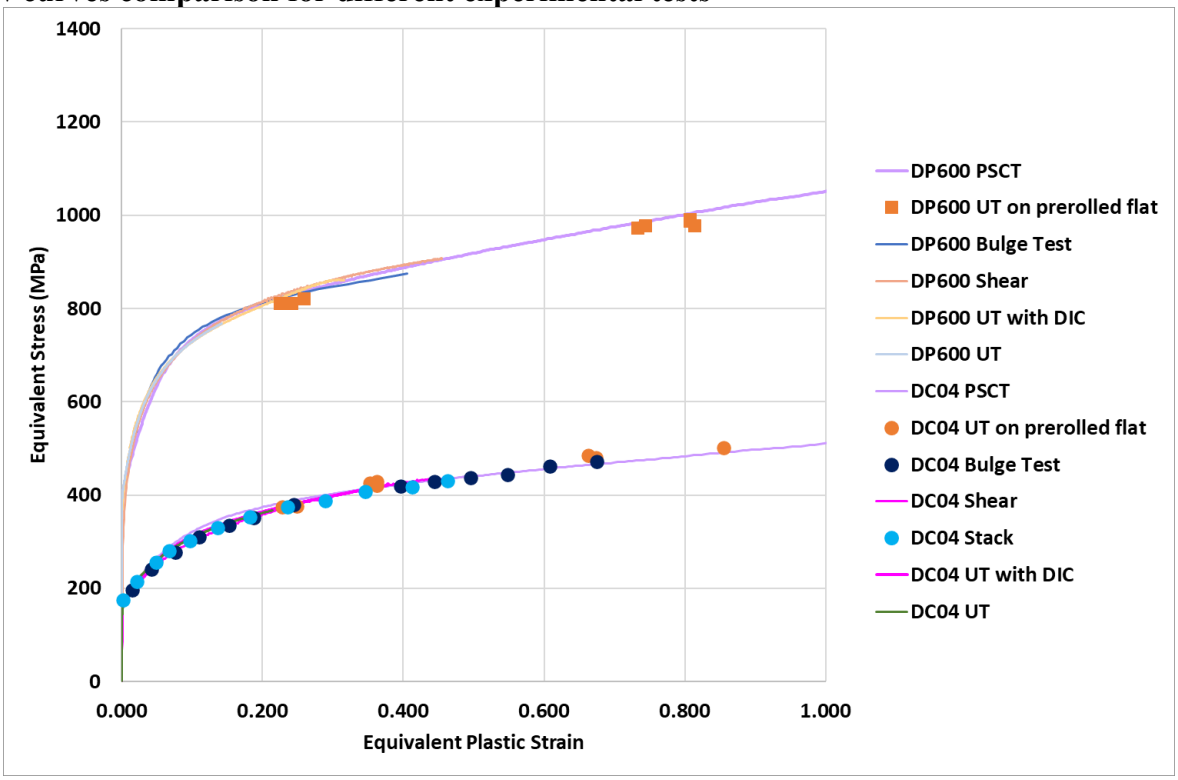

Figure 4 – True stress-plastic strain curves comparison for different steel grades and experimental tests

Figure 4 shows the true stress-plastic strain curves comparison for 2 different steel grades. As noted, beforehand, for several tests, the comparison of the flow curve with tensile flow curve needs to generate an equivalent stress-plastic strain curve. In this study, the generation of the equivalent stress-plasticity curve is based on a scalar multiplier parameter χ (Table 2) derived from the associated plasticity theory where the equivalent stress and equivalent strain are determined with plastic work per volume and the normality rule:

$$dW = d\varepsilon_{eq}^{p}\sigma_{eq} = d\varepsilon_{ij}^{p}\sigma_{ij} \text{ with } d\varepsilon_{ij}^{p} = \lambda\frac{\partial\sigma_{eq}}{\partial\sigma_{ij}} = \lambda V_{ij} \quad (2)$$

The χ-parameter value is not imposed with yield criterion, but it is defined by an inverse method to coincide the loading path flow curve with the uniaxial tensile flow curve like the HBT standardized procedure given by ISO 16808. For Von Mises material, the uniaxial tensile, the shear, the biaxial and plane strain compression χ-parameters are respectively equal to $\chi^{UT} = 1$, $\chi^{SH} = \sqrt{3}$, $\chi^{EEB} = 1$ and $\chi^{PSC} = -\sqrt{3}/2$.

Table 2 – Different Experimental Tests regarding Standard Uniaxial Tensile Test (Standard UTT)

Experimental tests	ε_{eq}^{p}	σ_{eq}
Standard UTT, UTT + DIC, UT on pre-rolled	$\frac{\varepsilon_{11}^{p}}{\chi^{UT}}$	$\chi^{UT}\sigma_{11}$
ST, ITT	$\frac{2\varepsilon_{12}^{p}}{\chi^{SH}}$	$\chi^{SH}\sigma_{12}$
SCT, HBT	$\frac{\varepsilon_{11}^{p}}{\chi^{EEB}}$	$\chi^{EEB}\sigma_{11}$
PSCT	$\frac{\varepsilon_{11}^{p}}{\chi^{PSC}}$	$\chi^{PSC}\sigma_{11}$

Isotropic hardening laws

Six isotropic hardening laws (Swift, Voce, SV, Exp_S, Exp_V and Exp_SV) are studied here based on three mathematical equations (Table 3). The isotropic hardening laws Exp_SV, Exp_S, Exp_V consist of considering the experimental points before the uniform elongation (UE) followed by the predictions of the mathematical equation at larger strain levels (Figure 5). The selection of experimental points before UE allows the Lüders plateau to be taken into account when it exists. For the selection of experimental points, Autoform® software imposes that the stress to be constinuously increasing. To identify the adjusting parameters, 3 different constraints are satisfied (Table 4):

- Constraint 1: the best approximation between the Yield Strength (YS) (or after Lüders plateau) and Ultimate Tensile Strength (UTS) points on the experimental flow curve issue of uniaxial tensile test (true stress-plastic strain curve).
- Constraint 2: the law passes through YS point (or low yield strength (LYS) if Lüders plateau).
- Constraint 3: Considère's criterion. At the point (UTS-UE), the Considère's criterion imposes that the slope of the true stress/true plastic strain curve is equal to the true stress at this point.

Table 3 – Different isotropic hardening laws

Name	Equation	Material Parameters
Swift (S)	$\sigma_{Swift} = K(\varepsilon_0 + \varepsilon)^n$ (3)	$K; n; \varepsilon_0$
Voce (V)	$\sigma_{Voce} = \sigma_0 + R_{Sat}\left(1 - exp(-C_r\varepsilon)\right)$ (4)	$\sigma_0; R_{Sat}; C_r$
Swift and Voce (SV)	$\sigma_{SV} = (1-\alpha)\sigma_{Swift} + \alpha\sigma_{Voce}$ (5)	$\alpha; K; n; \varepsilon_0; \sigma_0; R_{Sat}; C_r$

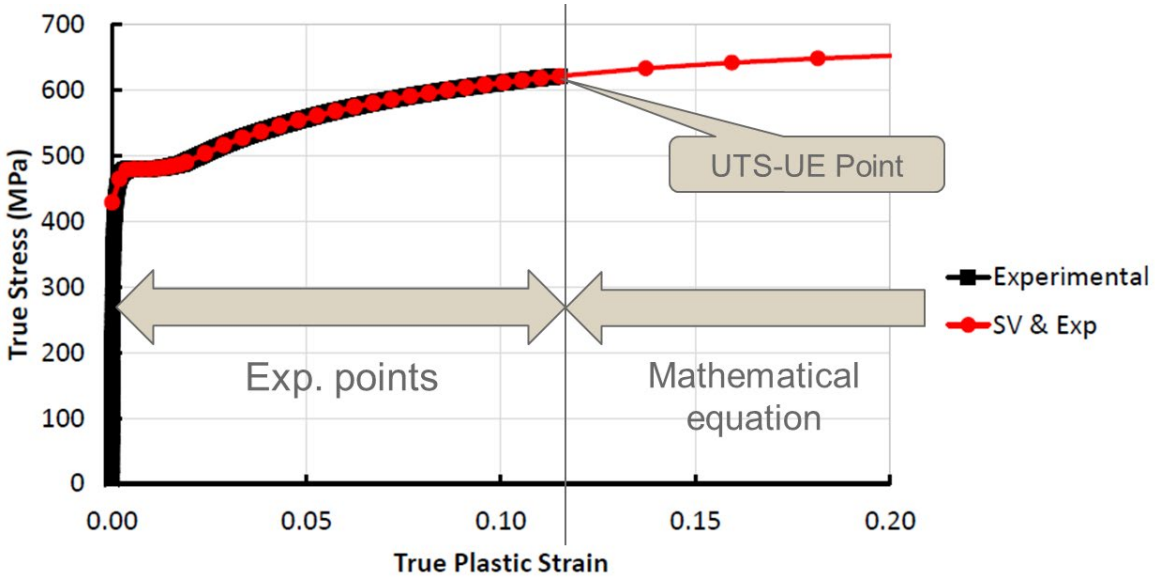

Figure 5 – The isotropic hardening laws Exp_SV, Exp_S, Exp_V consist of experimental points before UE and the mathematical equation after UE.

Table 4 – Constraints satisfied according to isotropic hardening laws.

Name	Constraint 1	Constraint 2	Constraint 3
Swift	Yes	Yes	No
Voce	Yes	Yes	No
SV	Yes	Yes	Yes
Exp_S	Yes	Yes	Yes
Exp_V	Yes	Yes	Yes
Exp_SV	Yes	Yes	Yes

Selection of the best isotropic hardening law.

For several comparison cases with experimental tests reaching large deformations, Figure 6 shows the ranking of these six isotropic hardening laws from first to sixth place. The ranking was based on the squared sum of stress deviations (Figure 7) between the mathematical law and experimental test measurements for several strain values after the uniform elongation point. The first place is the curve closest to the experimental curve (minimal squared sum) and the sixth place the furthest away (maximal squared sum) (Figure 8). According to our identification protocols, the best isotropic hardening law is Exp_S.

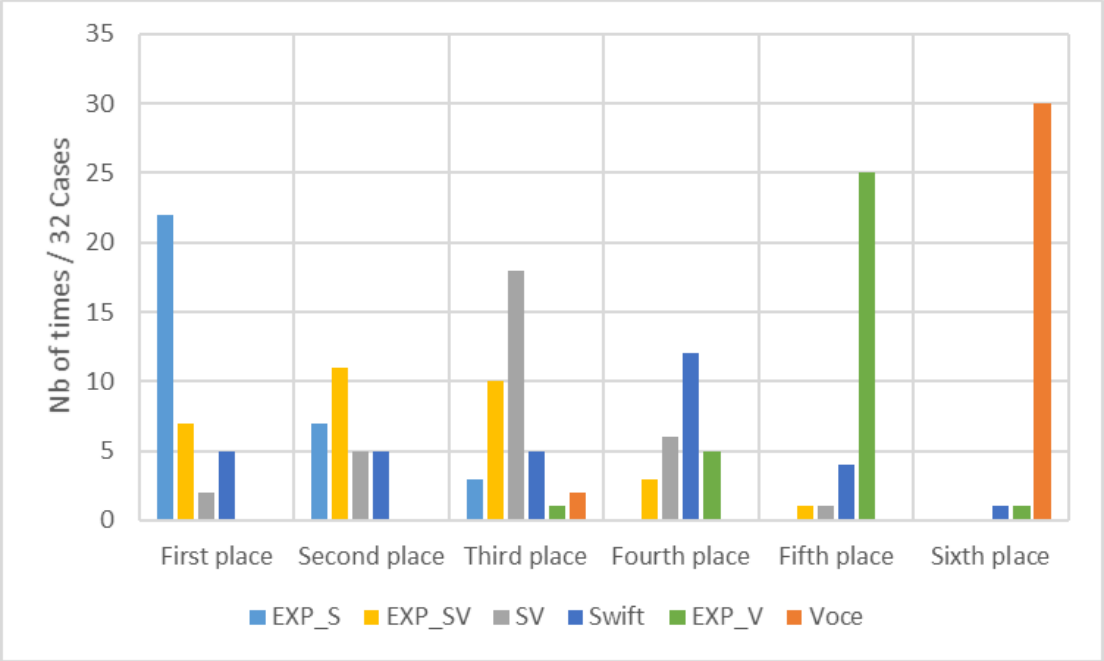

Figure 6 – Out of 32 cases of comparison, number of times the isotropic hardening law is in first, second … or sixth place.

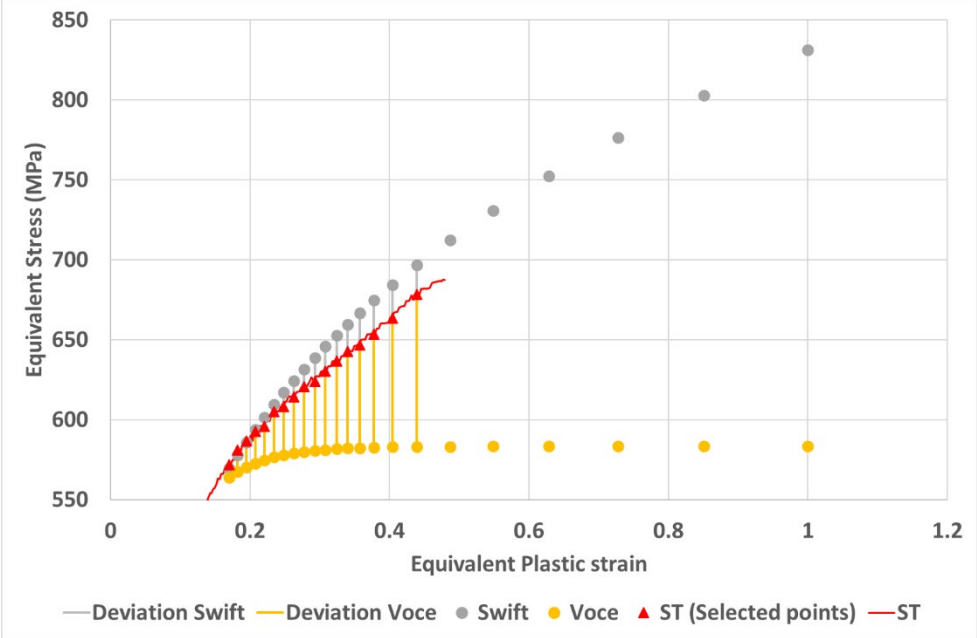

Figure 7 – For DP450 steel, Examples of stress deviations between the mathematical law and experimental test measurements for several strain values after the uniform elongation point.

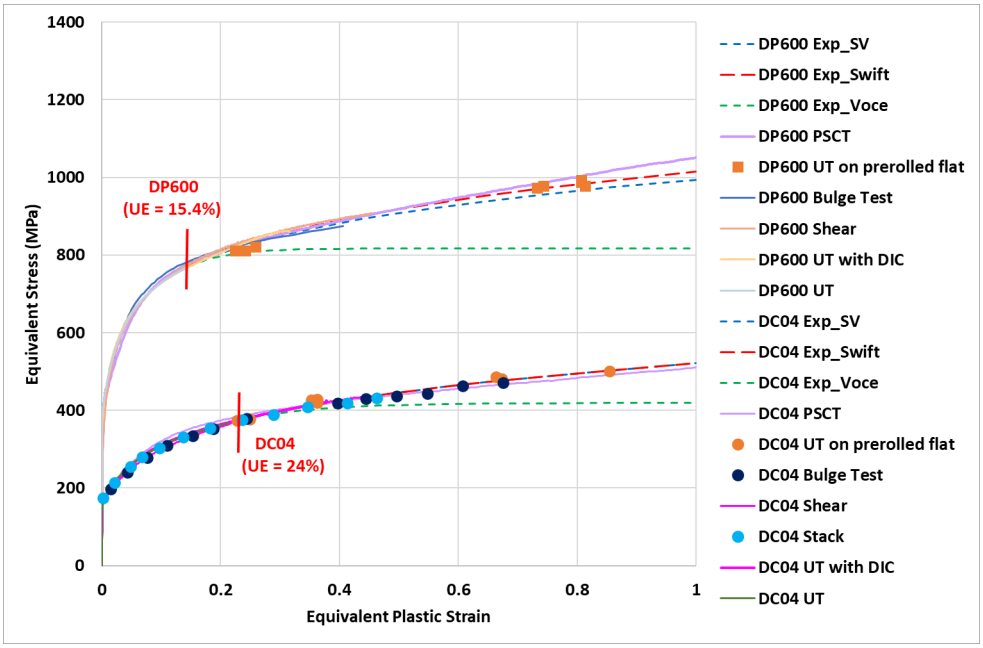

Figure 8 – Prediction/experience comparison of extended curves after uniform elongation defining the choice of isotropic hardening model.

Conclusions

Different experimental tests allowing to reach large strain have been presented: uniaxial tensile test with local measure, shear test, stack compression test, bulge test, in-plane torsion test, plane strain compression test and uniaxial tensile test on pre-rolled flat. The "Exp_S" isotropic hardening law is recommended for an accurate formability prediction in sheet forming numerical simulations, as soon as an adequate identification protocol, as proposed here, is used to determine the adjusting parameters.

References

[1] X. Lemoine, S. Sriram, R. Kergen, Flow Curve determination at large plastic Strain levels to accurately constitutive equations of AHSS in forming simulation, ESAFORM Conference 2011, Belfast, AIP publishing, https://doi.org/10.1063/1.3589715

[2] M. Jain, D.J. Lloyd, S.R. Macewen, Hardening laws, surface roughness and biaxial tensile limit strains of sheet aluminium alloys, Int. F. Mech. Sci. 38 (1996) 219-232.

[3] S. Dziallach, W. Bleck, M. Blumbach, T. Hallfeldt, Sheet metal testing and flow curve determination under Multiaxial conditions, Advanced Engineering Materials, 9 (2007) 987-994, https://doi.org/10.1002/adem.200700129

[4] S. Coppieters, H. Traphöner, F. Stiebert, T. Balan, T. Kuwabara, A.E. Tekkaya, Large strain flow curve identification for sheet metal, J. Mat. Proc. Techn. 308 (2022) 117725 https://doi.org/10.1016/j.jmatprotec.2022.117725

[5] M. Ben Tahar, Contribution à l'étude et la simulation du procédé d'hydroformage, PhD Report, Ecole des Mines de Paris, 2005

[6] X. Lemoine, E. Till, L. Kessler, T. Balan Improved constitutive equations for forming processes including ductility criteria, Technical Report EUR 22836 EN, Office for Official Publications of the European Communities, 2006.

[7] W. Bleck, S. Brühl, T. Gerber, A. Katsamas, R. Ottaviani, L. Samek, and S. Traint. Control and exploitation of the bake-hardening effect in multi-phase high-strength steels, Technical Report EUR 22448 EN, Office for Official Publications of the European Communities, 2006.

[8] M. Kleiner, V. Hellinger, M. Schikorra, L. Kessler, H.Vegter, D.Cornette, M Kulik and T. Brenne. Material parameters for sheet metal forming simulations by means of optimisation algorithms, Technical Report EUR 20907 EN, Office for Official Publications of the European Communities, 2003.

[9] C. Chermette, K. Unruh, I. Peshekhodov, J. Chottin and T. Balan. A new analytical method for determination of the flow curve for high-strength sheet steels using the plane strain compression test, Int. J. Mater Form, 13 (2019) 269–292. https://doi.org/10.1007/s12289-019-01485-4.

[10] H. Traphöner, T. Clausmeyer, and A.E. Tekkaya. Methods for measuring large shear strains in in-plane torsion tests, Journal of Materials Processing Tech. 287 (2021) 116516. https://doi.org/10.1016/j.jmatprotec.2019.116516

[11] H. Traphöner, T. Clausmeyer, S. Heibel and A.E. Tekkaya. Influence of manufacturing processes on material characterization with the grooved in-plane torsion test, Int. J. Mech. Sci. 146–147 (2018) 544–555. https://doi.org/10.1016/j.ijmecsci.2017.12.052

[12] V. Grolleau, C. Roth and D. Mohr. Design of in-plane torsion experiment to characterize anisotropic plasticity and fracture under simple shear, Int. J. Solids Struct. 236–237 (2022) 111314. https://doi.org/10.1016/j.ijsolstr.2021.111341

[13] M. Merklein, V. Gödel, Characterization of the flow behavior of deep drawing steel grades in dependency of stress state and its impact on FEA, ESAFORM Conference 2009, University of Twente, Netherland, Int J Mater Form 2 (Suppl 1), 415 (2009). https://doi.org/10.1007/s12289-009-0506-9

[14] Y.G. An, H. Vegter, Analytical and experimental study of frictional behavior in through-thickness compression test, Journal of Materials Processing Technology 160 (2005) 148–155. https://doi.org/10.1016/j.jmatprotec.2004.05.026

[15] M. Merklein, A. Kuppert, A method for the layer compression test considering the anisotropic material behavior, ESAFORM Conference 2009, University of Twente, Netherland, Int J Mater Form 2 (Suppl 1), 483 (2009). https://doi.org/10.1007/s12289-009-0592-8